

Experiment and modeling on the evaporation of β -diketonates of copper, yttrium and barium

Kan-Sen Chou *, Min-Jern Hwang and Ming-Yu-Shu

Department of Chemical Engineering, National Tsing Hua University, Hsinchu, Taiwan 30043 (Taiwan)

(Received 18 May 1993; accepted 8 June 1993)

Abstract

The evaporation behavior of the β -diketonates of copper, yttrium and barium were investigated in detail. The effects of sample characteristics and operating conditions, such as carrier gas flow rate, system pressure and temperature, and exposure area were studied. An empirical correlation, $n = k_2 L^{2/3} P^{-1} Q^{1/9} \exp(-\Delta H/RT)$, which is based on a simple mass transfer model is proposed to describe the rate of evaporation for these β -diketonates. The $L^{2/3}$ term represents the effects of the exposure area of the organometallic sample.

The calculated values agree well with our experimental data. The evaporation rate is, in general, very sensitive to temperature and system pressure, but not to gas flow rate. Another factor that influences the reproducibility of the evaporation is the stability of the material during storage. Storing the precursors below -10°C seems to help.

INTRODUCTION

The discovery of high temperature superconducting metal oxides, such as $\text{YBa}_2\text{Cu}_3\text{O}_{7-x}$ (YBCO), has stimulated an intense effort to produce them in thin films for microelectronics applications. Among the various approaches, the organometallic vapor phase epitaxy (OMVPE) is considered to have the potential to grow large-area, uniform films at a relatively high rate [1, 2]. Single-phase superconducting films of YBCO with critical superconducting temperature $T_c > 90\text{ K}$ and critical superconducting current J_c better than 10^6 A cm^{-2} have been successfully obtained in various laboratories around the world [3–5].

In spite of these successes, however, there are still some remaining problems to be solved before real applications [6, 7]. The stoichiometry control and reproducibility of grown films are two such problems. Part of the reasons for this situation, we believe, is due to the lack of a thorough understanding of the process mechanism. An OMVPE process can be divided into three basic steps: the evaporation of the organometallic (OM)

* Corresponding author.

precursors, the mixing and transport of these vapors to the substrate, and its decomposition and subsequent deposition as films. Our ability to control the compositions of grown films, therefore, relies on our ability to control the evaporation, transport, decomposition, and reaction processes.

Several studies on the evaporation of these β -diketonates, i.e. $Y(\text{thd})_3$, $\text{Cu}(\text{thd})_2$ and $\text{Ba}(\text{thd})_2$ (thd is tri(2,2,6,6-tetramethyl-3,5 heptanedione)) can be found in the literature [8–12]. Amano et al. [8] investigated the evaporation of $Y(\text{thd})_3$, and that of other lanthanides. Their emphasis was on obtaining equilibrium vapor pressures as a function of temperature for these compounds, as were the studies by Ozawa [9], Yuhya et al. [11] and Waffenschmidt et al. [12]. Zhang et al. [10], however, studied the effects of temperature, pressure and gas flow rates on the observed evaporation rates, although they did not suggest any explanation of their results. Schmaderer et al. [3] also studied the effect of temperature. Their data, however, showed a different temperature dependency from that of Zhang et al. [10]. Therefore, we feel that there is still a need to examine this evaporation process to gain more understanding. Here we report not only experimental results, but also offer a quantitative explanation based on a simple mass transfer model. A correlation equation, which fits well with our data, is proposed to relate the evaporation rate with various process variables. This empirical equation should be helpful in the design and control of a future OMVPE process for growing YBCO films.

EXPERIMENTAL

The metal β -diketonates used, $Y(\text{thd})_3$, $\text{Ba}(\text{thd})_2$ and $\text{Cu}(\text{thd})_2$, were obtained from Strem Chemicals Inc. Both $Y(\text{thd})_3$ and $\text{Cu}(\text{thd})_2$ were supplied as large crystals that were ground to smaller particles before use. $\text{Ba}(\text{thd})_2$ was already a fine powder and was therefore used as received.

Evaporation experiments were conducted in a simple horizontal tube reactor, heated by a resistance heater. The organometallic (OM) powders were placed in a small cell with an open area of 2.8 cm^2 . We then placed the cell in the constant temperature zone of our tube evaporator. Argon was used as the carrier gas, whose flow rate was controlled by a mass flow controller. The rate of evaporation was calculated from the weight loss after each run, which was kept at 30 min for this work. The parameters that were investigated included: evaporation temperature and pressure, carrier gas flow rate, and the exposure areas of the OM precursors.

Argon gas was passed over tetrahydrofuran (THF) before entering the evaporator [3] to improve the stability of evaporation of $\text{Ba}(\text{thd})_2$. We also repeated evaporation runs under the same conditions for $Y(\text{thd})_3$ and $\text{Cu}(\text{thd})_2$ to check the reproducibility of this process. It is important to maintain good reproducibility if this process is ever going to be used in real applications.

In addition to those in the horizontal evaporator, we also carried out some experiments in a Cahn balance (Model C2000) which operated as a vertical tube reactor. This equipment gave a rapid determination of the dynamic evaporation behavior.

RESULTS AND DISCUSSION

A simple model for mass transfer

Our purpose here is to develop a working relationship between the evaporation rate and the operating parameters, i.e. the temperature, pressure and carrier gas flow rates. The phenomenon of molecules evaporating into a flowing carrier gas from a fixed source may be described by a simple mass transfer equation

$$n = K_c A \Delta C \quad (1)$$

Where K_c is the effective mass transfer coefficient, A is the apparent exposure area of the sample (taken here as $W \times L$ where W and L are the equivalent width and length of the sample cell) and ΔC is the concentration gradient for mass transfer. If we assume saturated vapor pressure at the surface of the source sample and zero concentration in the bulk carrier gas, this ΔC term simply becomes the saturated concentration of vapor molecules at the experimental temperature, i.e.

$$\Delta C = C_s = P_s/RT \quad (2)$$

where P_s is the saturated vapor pressure which can be expressed as

$$P_s = P_s^* \exp(-\Delta H/RT) \quad (3)$$

The ΔH term would therefore refer to the enthalpy of evaporation for the species in question.

We then need to choose an appropriate correlation equation from the literature for evaluating K_c for our case. K_c should in general reflect the effects of fluid flow and, thus, the reactor geometry. After some trials, the following empirical correlation (eqn. (4)) was considered the most appropriate for our horizontal evaporator. Our equation is similar to the Leveque expression for laminar flow in tubes [11]. The only difference is in the exponent of Re which was $1/9$ in our case and $1/3$ in the Leveque equation

$$Sh = K_c d/D = k_1 Re^{1/9} Sc^{1/3} (W/L)^{1/3} \quad (4)$$

where Sh is the Sherwood number, Re the Reynold number ($= \rho v d/\mu$), Sc

the Schmidt number ($= \mu/(D\rho)$), D the diffusion coefficient of the species in the carrier gas, ρ and μ the density and viscosity of the vapor phase (argon), and d the diameter of tube evaporator. A value of 1/9 for the exponent of the Re number was found to give a much better fit than the conventional value 1/3 of laminar flow in a circular tube.

Furthermore, the diffusion coefficient can be simplified for ease of calculation

$$D = D_0(T/300)^{1.75}(760/P) \quad (5)$$

D_0 can be considered as the diffusion coefficient at 300 K and 760 Torr. The exponent of temperature term in Eqn. (5) was found to have insignificant influence on the calculated rates of evaporation. Because this value is often between 1.5 and 2.0 [11], it is therefore fixed at the intermediate value of 1.75 in our calculation.

Because the readout from a mass flow controller is expressed under STP conditions, we need to convert it to the actual conditions in the evaporator, i.e.

$$Q = Q_{\text{stp}}(T/273)(760/P) \quad (6)$$

Units for temperature and pressure are kelvin and torr respectively. The average velocity, i.e. v , can then be obtained by simply dividing Q by the cross-sectional area for the gas flow. By substituting eqns. (2)–(6) into eqn. (1), we can then express the rate of evaporation in terms of Q , T , P and the dimensions of the sample cell as follows

$$N = k_2 W^{4/3} L^{2/3} T^{2/3} P^{-1} Q_{\text{stp}}^{1/9} \exp(-\Delta H/RT) \quad (7)$$

The constant k_2 contains the effects of P_s^* , D_0 , d (diameter of tube), and other constants. The effect of the $T^{2/3}$ term is negligible when compared with the Arrhenius temperature dependency. We can thus include this factor in the constant (k_2) term. This correlation should hold for other types of evaporator as well, except that the fitted parameters may be different.

Effects of sample area

At first sight, eqn. (1) seems to suggest that the rate of evaporation is directly proportional to the “exposure area” (defined as the cross-sectional area of the sample cell in the direction of flow, $W \times L$). The final correlation (eqn. (7)), however, shows that the evaporation rate is actually proportional to $W^{4/3}$ and $L^{2/3}$. Nevertheless, one may wonder whether the total surface area of the particulate sample is also an important factor. The experimental conditions and data for $\text{Cu}(\text{thd})_2$ listed in Table 1 are

TABLE 1

Experimental conditions and results illustrating the effects of exposure area and surface area of Cu(thd)₂ samples

Run	Sample weight/g	Particle size/mm	No. of cells	Evaporation rate/ $\times 10^{-5}$ mol h ⁻¹ ^a
1	0.2308	≈0.10	2	5.55
2	0.2308	≈2.0	2	5.33
3	0.2313	≈6.0	2	4.50
4	0.2116	≈2.0	1	3.47
5	0.2174	≈6.0	1	3.28

Other experimental conditions were: Ar flow rate, 13.5 sccm; pressure, 10 Torr; temperature, 125°C.

^a Average from two runs.

intended to address this question. The Cu(thd)₂ sample was supplied as large crystals about 6 mm in size. It was ground in an agate mortar to increase its specific surface area. A few smaller crystals (about 2 mm) were picked out before the sample was finally ground to the 0.05–0.1 mm size range. Using the same weight of differently sized samples (shown as Runs 1–3 in Table 1) provided different total powder surface areas but the same “exposure area” because the same number of cells were used. The evaporation rates were different: the smallest particles showed the highest evaporation rate due to its largest total surface area. These results suggest that the total surface area (specific surface area \times sample weight) does have some effect on the evaporation rate. Conceivably, when the OM powders were put into the sample cell, the top layer of particles would contribute most to the evaporation rate. Contributions from particles underneath would become less if they were more densely packed in the sample cell. A quantitative analysis of this effect requires further studies.

Next we changed the exposure area by putting approximately the same amount of sample in one cell instead of two, i.e. Runs 4 and 5 versus 2 and 3. The sample length in Runs 4 and 5 is then twice that of the corresponding samples in Runs 2 and 3. The observed ratios of the respective evaporation rates for Run 2/Run 4 (2 mm particle size) and Run 3/Run 5 (6 mm particle size) are 1.54 and 1.37. The predicted ratio from eqn. (7) is 1.59, i.e. $2^{2/3} = 1.59$. The deviation for samples of 6 mm was probably due to the fact that the number of particles of this size was too low to fill the two cells completely. In other words, the effective sample length for two-cell runs here is less than $2L$, and the ratio of the evaporation rates is consequently smaller than the predicted value of 1.59, i.e. only 1.37. To avoid any confusion, we therefore used the same amount of sample, i.e. the same particle size and the same number of cells for all subsequent runs.

Effects of operating conditions

In this section, we discuss the effects of operating conditions, namely the carrier gas flow rate, and the operating pressure and temperature. The experimental results are compared with those calculated using our simple model. The respective empirical equations adopted for $\text{Cu}(\text{thd})_2$ and $\text{Y}(\text{thd})_3$ are

$$\text{Cu}(\text{thd})_2 \quad n = (3.24 \pm 0.55) \times 10^{12} L^{2/3} P^{-1} Q^{1/9} \exp(-14840/T) \quad (8)$$

$$\text{Y}(\text{thd})_3 \quad n = (3.88 \pm 0.47) \times 10^{13} L^{2/3} P^{-1} Q^{1/9} \exp(-16450/T) \quad (9)$$

Units for these parameters are: n in mol h^{-1} ; L in cm; P in Torr; Q in sccm; T in K. The proportional constants were determined from all data. No such correlation could be proposed for $\text{Ba}(\text{thd})_2$ due to insufficient data.

Effect of carrier gas flow rate

Figure 1 shows the results of Ar flow rate versus measured evaporation rate for both $\text{Cu}(\text{thd})_2$ and $\text{Y}(\text{thd})_3$. The dependency of n on Q is only to its power of $1/9$, compared to $1/3$ for other correlations in the literature [13]. This low value of the exponent suggests that forced convection is not very important for our evaporator. One possible reason is probably the very low pressure used in our experiments, i.e. 10–80 Torr, compared to atmospheric conditions used in others. The much lower density of gas molecules would decrease the convection effect. The small discrepancy between simulation and experimental data shown in Fig. 1 is primarily caused by the proportional constant. It is also possible that some deviation originates from the stability of the sample itself [14], as discussed below.

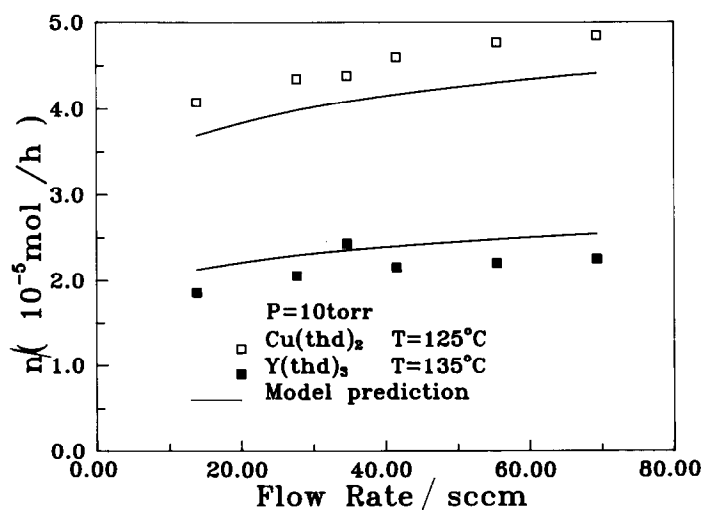


Fig. 1. Effects of argon flow rate on the rate of evaporation for $\text{Cu}(\text{thd})_2$ and $\text{Y}(\text{thd})_3$. The solid curves represent calculated results from empirical correlations.

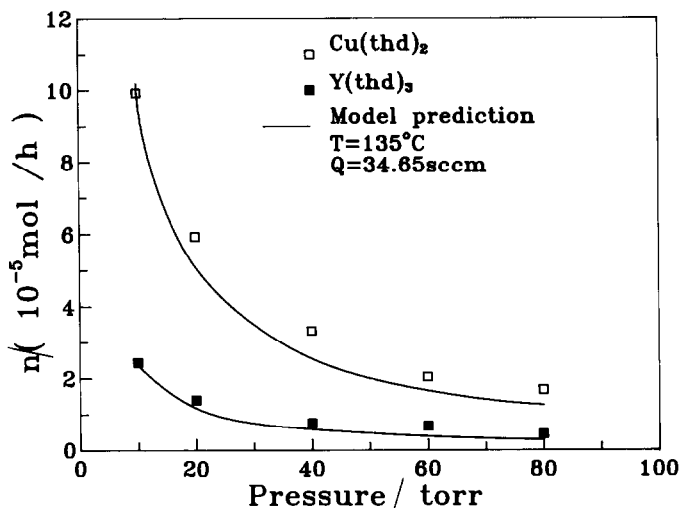


Fig. 2. Effects of system pressure on the rate of evaporation for $\text{Cu}(\text{thd})_2$ and $\text{Y}(\text{thd})_3$. The solid curves are from our correlations.

Effect of operating pressure

Figure 2 shows the evaporation rates at different operating pressures. They change inversely with pressure and can be predicted quite well by our model. This inverse relationship is basically the result of the inverse dependency of the diffusion coefficient on the system pressure, while the mass transfer coefficient is directly proportional to the diffusion coefficient.

Effect of temperature

The plots of evaporation rates versus $1/T$ are shown in Fig. 3. A linear relationship is observed for all three cases. Although our model predicts only a weak dependency on temperature for the pre-exponential term, the data can still be fitted by the Arrhenius equation due to the narrow temperature range applied. An equivalent enthalpy of evaporation for the OM precursors can be derived from the slope. We also carried out the same runs in a micro-balance and obtained similar results. The ΔH values obtained from both series of runs, together with the literature data, are listed in Table 2. The agreement between our data sets is satisfactory. However, some discrepancy can be noted between our data and the literature values. The reasonable agreement between our data and that of ref. 12 is surprising, because quite different experimental techniques were employed.

Figure 4 shows the evaporation rates of $\text{Ba}(\text{thd})_2$ taken from the microbalance as a function of time. The rates decrease continuously for pure $\text{Ba}(\text{thd})_2$. This trend was quite consistent from run to run. As a result,

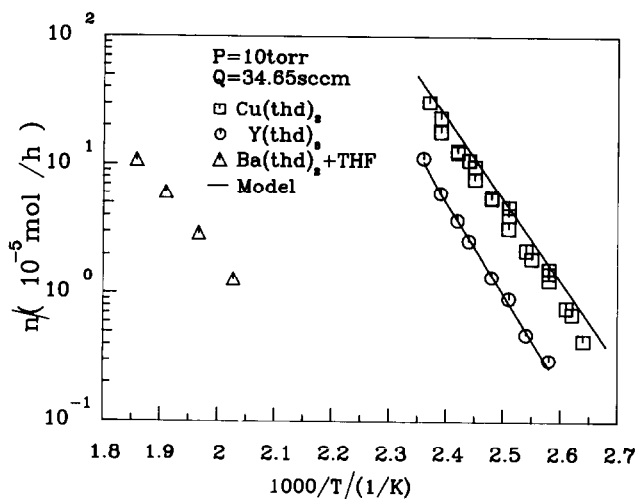


Fig. 3. Plots of evaporation rate versus $1/T$ for Y, Cu and Ba β -diketonates. Linear Arrhenius relationships are observed for these OM precursors.

the average evaporation rates from the horizontal evaporator are approximately the same. No attempt, however, was made to obtain n versus $1/T$ data for this case. The decreasing trend could be diminished by including THF vapor in the Ar flow. The $\ln(n)$ versus $1/T$ plot obtained from the horizontal evaporator also produced a linear relationship. The averaged ΔH values are $25.8 \text{ kcal mol}^{-1}$ for $\text{Ba}(\text{thd})_2 + \text{THF}$, $29.7 \text{ kcal mol}^{-1}$ for $\text{Cu}(\text{thd})_2$, and $32.9 \text{ kcal mol}^{-1}$ for $\text{Y}(\text{thd})_3$.

Sensitivity analysis

The sensitivity of the evaporation rate to these process variables can be easily evaluated from eqn. (7). By differentiating n with respect to T , P and

TABLE 2

ΔH values (kcal mol^{-1}) for evaporation of β -diketonates

Sample	Literature data ^a					Our data	
	[3]	[8]	[10]	[11]	[12]	Evaporator	Balance
$\text{Y}(\text{thd})_3$	24.4	37.5	12.6	32.5	19.9	32.7	33.1
$\text{Cu}(\text{thd})_2$	18.3	–	21.8	25.4	29.5	29.5	29.9
$\text{Ba}(\text{thd})_2 + \text{THF}$	–	–	–	–	–	25.0	26.7
$\text{Ba}(\text{thd})_2$	23.4	–	13.4	–	16.5	–	–

Operating conditions: for our data, 10 Torr and 34.6 sccm of Ar; ref. 3; 10 mbar and 417 sccm; and ref. 10, 50 Torr and 125–1000 sccm.

^a Data from refs. 3 and 10 were read from their corresponding figures; data from ref. 8 were from a table.

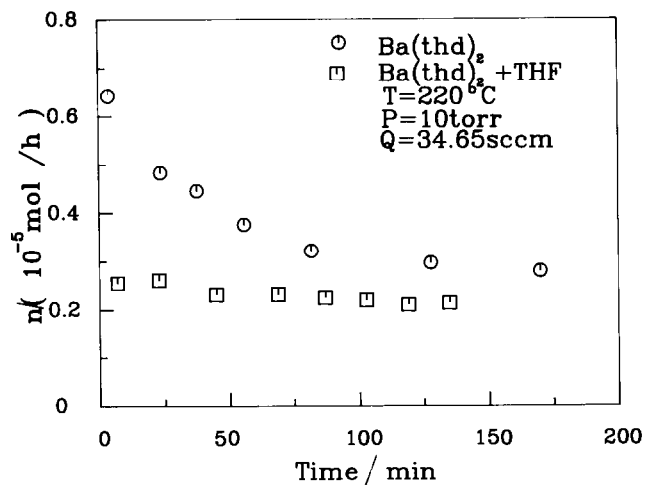


Fig. 4. Comparison of rate of evaporation of $\text{Ba}(\text{thd})_2$ with or without the inclusion of THF vapor in the carrier gas. These runs were made in a Cahn microbalance.

Q and then dividing by n , we obtain

$$(dn/dT)/n = \Delta H/RT^2 \quad (10)$$

$$(dn/dP)/n = -1/P \quad (11)$$

$$(dn/dQ)/n = 1/(9Q_{\text{stp}}) \quad (12)$$

Taking $\text{Cu}(\text{thd})_2$ as an example, its approximate ΔH value is 30 kcal mol^{-1} . Then at $T = 120^\circ\text{C}$, $P = 10 \text{ Torr}$ and $Q = 40 \text{ sccm}$, the percentage change in n will be 9.8% per K, -10% per Torr and 0.3% per sccm, respectively. Evidently, the rate of evaporation is least sensitive to the carrier gas flow rate, with about the same degree of sensitivity to temperature and pressure. Both the temperature and gas flow rate are controlled in our present system, but not the pressure, which was only monitored. The pressure was adjusted manually when the reading deviated by more than 2–3 Torr from the set-point. The reactor pressure usually rose slowly during the experiments. Either the release of entrapped solvent molecules or the decomposition of β -diketonates (especially for $\text{Ba}(\text{thd})_2$) could cause this increase in pressure. The above analysis indicated the importance of controlling the system pressure in order to obtain a more reproducible, more stable evaporation rate.

Figure 5 shows the results of some repeated runs using as-received samples that were simply stored in a desiccator. The averages and standard deviations for $\text{Cu}(\text{thd})_2$ and $\text{Y}(\text{thd})_3$ are $(4.50 \pm 0.41) \times 10^{-5} \text{ mol h}^{-1}$ and $(1.49 \pm 0.11) \times 10^{-5} \text{ mol h}^{-1}$ respectively. $\text{Y}(\text{thd})_3$ showed slightly better reproducibility over $\text{Cu}(\text{thd})_2$. The same observation was also noted from eqns. (8) and (9). In addition to the process variables, we believe that the

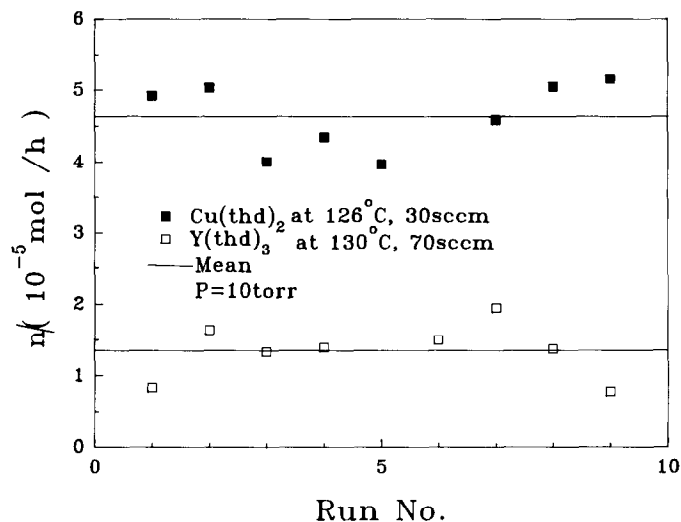


Fig. 5. Batch to batch variation of evaporation rates for repeat runs using as-received $\text{Cu}(\text{thd})_2$ and $\text{Y}(\text{thd})_3$.

effect of material stability should also be considered when we assess the reproducibility of these evaporation rates [14]. To prevent any possible changes during storage, we then recrystallized these particles in THF, dried them at 80°C overnight (to remove entrapped solvent) and stored them at -10°C in Ar. The reproducibility improved quite considerably as shown by the results in Fig. 6. The averages and standard deviations are $(4.42 \pm 0.09) \times 10^{-5}$ and $(1.13 \pm 0.036) \times 10^{-5} \text{ mol h}^{-1}$ respectively.

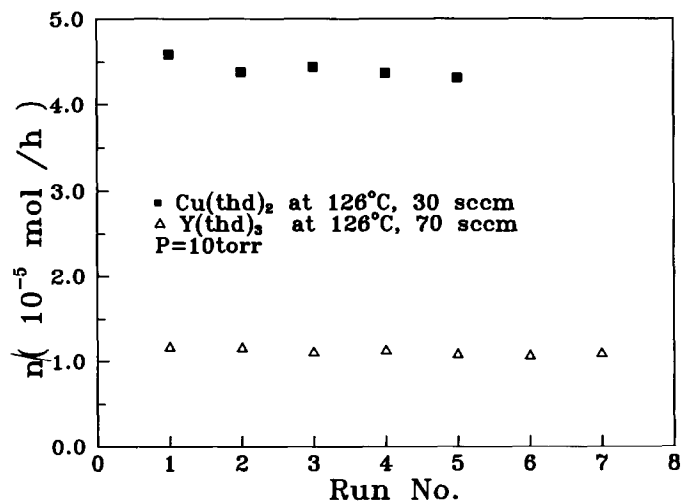


Fig. 6. Similar reproducibility test to that shown in Fig. 5, except that the samples were recrystallized, dried and stored below -10°C .

CONCLUSION

From the results presented above, we can conclude that the rate of evaporation depends not only on the obvious operating parameters, but also on other physical characteristics of the system. Therefore, the sample characteristics, such as particle size and sample quantity, the geometry of the evaporator and sample cell, and the conditions of evaporation (T , P and Q) all exhibit some effect on the results. An empirical correlation derived from a simple mass transfer model, $n = kL^{2/3}P^{-1}Q^{1/9} \exp(-\Delta H/RT)$ was found to fit very well with our data for $\text{Cu}(\text{thd})_2$ and $\text{Y}(\text{thd})_3$ from the horizontal evaporator. The evaporation rate of $\text{Ba}(\text{thd})_2$ can be stabilized by including THF vapors in the Ar carrier gas. The ΔH values were found to be 25.8, 29.7 and 32.9 kcal mol⁻¹ for $\text{Ba}(\text{thd})_2 + \text{THF}$, $\text{Cu}(\text{thd})_2$ and $\text{Y}(\text{thd})_3$, respectively.

A subsequent sensitivity analysis indicated the importance of both the temperature and pressure of the system in maintaining a stable rate of evaporation. The deviation in pressure during the experiments was probably one of the reasons for the observed deviation in evaporation rates. The shelf stability of these OM precursors is another possible reason. Storage below 0°C seems to improve the stability of these OM compounds.

ACKNOWLEDGMENT

The authors thank National Science Council of ROC for financial support of this research work, grant no. NSC 81-0511-M007-507.

REFERENCES

- 1 M. Schieber, J. Crystal Growth, 109 (1991) 401–407.
- 2 A. Feng, L. Chen, T.W. Piazza, H. Li, A.E. Kaloyeros, D.W. Hazelton, L. Luo and R.C. Dye, Appl. Phys. Lett., 59(10) (1991) 1248–1250.
- 3 F. Schmaderer, R. Huber, H. Oetzmann and G. Wahi, Appl. Surface Sci., 46 (1990) 53–60.
- 4 R. Hiskes, S.A. DiCarlios, J.L. Young, S.S. Laderman, R.D. Jacowitz and R.C. Taber, Appl. Phys. Lett., 59(5) (1991) 660–607.
- 5 T. Hirai and H. Yamane, J. Crystal Growth, 107 (1991) 683–691.
- 6 H.J. Scheel, M. Berkowski and B. Chabot, J. Crystal Growth, 115 (1991) 19–30.
- 7 H. Harima, H. Ohnishi, K.I. Hanaoka, K. Tachibana and Y. Goto, Jpn. J. Appl. Phys., 30(9A) (1991) 1946–1955.
- 8 R. Amano, A. Sato and S. Suzuki, Bull. Chem. Soc. Jpn., 54 (1981) 1368–1374.
- 9 T. Ozawa, Thermochim. Acta, 174 (1991) 185–199.
- 10 K. Zhang, B.S. Kwak, E.P. Boyd, A.C. Wright and A. Erbil, in R.D. McConnel and S.A. Wolf (Eds.), Science and Technology of Thin Film Superconductors, Plenum Press, New York, 1989, pp. 271–279.
- 11 S. Yuhya, K. Kikuchi, M. Yoshida, K. Sugawara and Y. Shiohara, Mol. Cryst. Liq. Cryst., 184 (1990) 231–235.

- 12 E. Waffenschmidt, J. Musolf, M. Heuken and K. Heime, *J. Superconductivity*, 5(2) (1992) 119–125.
- 13 A.H.P. Skelland, *Diffusional Mass Transfer*, Wiley–Interscience, New York, 1974.
- 14 T. Hashimoto, H. Koinuma, M. Nakabayashi, H. Shiraishi, Y. Suemune and T. Yamamoto, *J. Mater. Res.*, 7(6) (1992) 1336–1340.